Wenzhen Huang
Dept. of Mechanical Engineering,
University of Massachusetts,
Dartmouth, MA 02747
e-mail: whuang@umassd.edu

Jijun Lin
Engineering Systems Division,
School of Engineering,
Massachusetts Institute of Technology,
Cambridge, MA 02139-4307
e-mail: jijunlin@mit.edu

Michelle Bezdecny
GE Global Research Center,
Niskayuna, NY 12309
e-mail: bezdecny@research.ge.com

Zhenyu Kong
School of Industrial Engineering and Management,
Oklahoma State University,
Stillwater, OK 74078
e-mail: james.kong@okstate.edu

Dariusz Ceglarek
Department of Industrial and Systems Engineering,
University of Wisconsin-Madison,
Madison, WI 53706
e-mail: darek@engr.wisc.edu

Stream-of-Variation Modeling—Part I: A Generic Three-Dimensional Variation Model for Rigid-Body Assembly in Single Station Assembly Processes

A stream-of-variation analysis (SOVA) model for three-dimensional (3D) rigid-body assemblies in a single station is developed. Both product and process information, such as part and fixture locating errors, are integrated in the model. The model represents a linear relationship of the variations between key product characteristics and key control characteristics. The generic modeling procedure and framework are provided, which involve: (1) an assembly graph (AG) to represent the kinematical constraints among parts and fixtures, (2) an unified method to transform all constraints (mating interface and fixture locators etc.) into a 3-2-1 locating scheme, and (3) a 3D rigid model for variation flow in a single-station process. The generality of the model is achieved by formulating all these constraints with an unified generalized fixture model. Thus, the model is able to accommodate various types of assemblies and provides a building block for complex multistation assembly model, in which the interstation interactions are taken into account. The model has been verified by using Monte Carlo simulation and a standardized industrial software. It provides the basis for variation control through tolerance design analysis, synthesis, and diagnosis in manufacturing systems.
[DOI: 10.1115/1.2738117]

1 Introduction

1.1 Problem Description. Modern manufacturing systems involve multiple operations in multistation processes. Typical examples include automotive body assembly, aerospace and shipbuilding manufacturing, etc. For example, automotive body assembly is typically composed of about 60 assembly stations, 150–250 sheet metal parts, and thousands of locating, clamping, and welding points. Dimensional variation in these systems has been identified as a critical quality issue. It contributes to over two-thirds of the dimensional quality problems in the assembly processes in automotive and aerospace industries [1]. Therefore, the stream-of-variation analysis (SOVA) has attracted more and more interest from both the industrial and academic communities in the last decade [1–12].

Product-dimensional quality control, which includes variation propagation modeling, tolerance analysis and synthesis, and variation reduction during manufacturing phase, plays a critical role for the success of a manufacturing enterprise. However, the inherent complexity in these processes makes it very challenging to model and predict the stream of variation.

The scope of the paper is confined to the three-dimensional (3D) rigid model, which is the first step and will provide an important model component in system level modeling. The ultimate goal of the research is to establish a comprehensive methodology, through the integration of the rigid and compliant models, for variation modeling and analysis at the system level.

In general, the variation propagation in rigid-body assemblies is driven by three fundamental mechanisms: (1) part-to-part interactions, (2) part-to-fixture interactions, and (3) interstation interactions which are in fact a specific type of (2) between stations. A two-step bottom-up strategy is proposed toward the ultimate goal of system-level modeling: station-level modeling and multistation system level modeling. As the first step, the station-level modeling is addressed in this paper.

In type I assembly (i.e., all the parts are positioned by other mating parts in the assembly), there are only the part-to-part interactions, whereas for type II assembly (i.e., the parts are positioned by both fixtures and other parts), both part-to-part and part-to-fixture interactions exist. Both interactions have been identified by industry as the two most frequent causes of engineering changes [13]. In automotive body assembly, the part-to-fixture interaction has been a dominant contributor to dimensional quality problems [1,5,8]. In the single-station cases, only the local effects of variation factors (first two types of the interactions) come into play, whereas the transition effect of the interstation interaction needs to be considered only in multistation processes. The types of mating interfaces/joints and respective geometric errors are key factors in the variation modeling. Fixture errors and layout are key factors for both dimensional variation and locating stability. In general, under rigid-body assumption, the interaction between parts should be considered as kinematics constraints, i.e., interactions between imperfect surfaces or contacts between random surfaces. Therefore, the part-to-part interaction involves complex kinematics interactions because of the joint types and the intrinsic nature of random geometric errors on them. The part-to-fixture interaction is customarily considered as a point contact interaction among part surfaces and locators. The variation stack up can thus

Contributed by the Manufacturing Science Division of ASME for publication in the JOURNAL OF MANUFACTURING SCIENCE AND ENGINEERING. Manuscript received August 14, 2006; final manuscript received February 28, 2007. Review conducted by Shivakumar Raman. Paper presented at the 2006 International Conference on Manufacturing Science and Engineering (MSEC2006), October 8–11, 2006, Ypsilanti, MI.

Table 1 Summary of type-1 and type-2 assemblies

	Only mating feature (type I)	Only fixture	Fixture and mating feature (type II)
Form closure	[8,12,14,15]	[3,8,11,18,26,27,29,30]	Proposed in this paper
Force closure	[23]	[6]	

be formulated by a simple kinematics transformation. To achieve generality all the possible combinations of interactions need to be considered.

Therefore, the interaction model for a single assembly station can be formulated as a method to characterize different interactions in a unified framework.

1.2 Related Works. Comprehensive research has been conducted in the last two decades in modeling rigid assembly for tolerancing and variation analysis [14–16]. The kinematics joint concept has been applied to define kinematical constraints of mating features. Kinematics principles and transformations are the major approaches for formulating error stackup between parts. A comprehensive review was given recently [16]. The emphasis was on an error stack up model of type I assembly problems, in which positions of parts were exclusively determined by their mating features. The modeling techniques for type I assembly are product-information oriented, i.e., the effects of process factors, such as fixture locating errors and interstation interaction are not included in the models.

Methods for SOVA analysis in type II problems were also developed, in which the positions of parts were dependent on both mating features and fixtures. Type II assembly is common in automotive and aircraft industries, where parts are located and fixed by fixtures, and then welded or riveted. A special case in the type II can be found in machining, where the part is positioned by fixture, exclusively. A comprehensive review on error stack-up analysis involved in a single machining process can be found in [17]. A linear model for the error stack-up analysis in a single machining station was developed in [18,19], which includes the contact geometry between locators and parts. A variation propagation state-space model in a multistage machining process was developed in [20,21], in which both the local impact and the interstation interaction of the variation factors from fixtures were included. The emphasis was on the fixture locating errors in machining, since machining does not involve interaction effect among part mating features.

Efforts have been made in SOVA modeling in multistation assembly processes (Table 1). The state-space model was initially introduced for variation propagation analysis in [11]. In a similar vein, [12] adopted the Markov state transition concept to create a state transition model to describe the variation propagation in assembly processes. The quality state was defined as the deviations of parts in an assembly, which were produced from variation factors at each station and transmitted through the system. These models took advantage of the well-established techniques in modern control theory for design analysis, monitoring, and diagnosis. These works constructed the framework for the recent research in [2,8,22,23]. In [8], the state space model was applied to the two-dimensional (2D) rigid assembly process for design evaluation, tolerance analysis, and diagnosis. Lap joint, fixture error, and interstation interaction of fixture locating errors were considered to perform 2D (in-plane) analysis. A comprehensive review of the 2D state-space model and its applications in automotive assembly can be found in [2].

Data-driven models were developed for dimensional variation diagnosis. [3,24] used an AR(1) model to investigate dimensional variation in the assembly process as well as in the machining process. They identified interrelations between their statistical model and the physical process by estimating the parameters of the AR(1) model based on the real process measurements.

Recently, some attempts were also made to model compliant assemblies [4,6,9,25–28]. Elastic deformation and locked-in stresses created in closing the gaps among the parts were analyzed by using mechanics principles and finite element analysis (FEA). Linear FEA model [6] and nonlinear contact FE model [4] were developed to build numerical models for deformation analysis. Camelio [28] tried to directly extend the state-space model to compliant assembly systems. In that model, the quality state was defined as deformation of nodes in FEA analysis.

In spite of tremendous efforts in SOVA modeling in the last decade [1–12,20,21], the developed models are still limited for comprehensive variation analysis of real manufacturing systems. Neither well-established models nor emerging techniques are available for modeling the generic 3D type-II assembly process in multistation assembly systems. The comparison of available models is summarized in Table 1.

In this paper, a methodology is developed to create a generic 3D rigid-body assembly variation propagation model in single-station assembly processes. This work provides a basis for subsequent system level modeling. The most recent work of a 3D rigid-body SOVA model in a multistation assembly processes is presented in [22].

1.3 Proposed Method. The paper is organized as follows. In Sec. 2, the assumptions of the model are introduced and the major variation factors are identified. In Sec. 3, the concept of a generic *virtual fixture* model is presented, by which an explicit formula for variation analysis is derived. In Sec. 4, an elementary model for variation flow between two parts is initially derived and then a modeling method is proposed for integrating kinematical constraints of generic joints and fixtures in a unified framework of the *generalized virtual fixture*. Afterward, the 3D rigid assembly model for variation prediction in a single-station system is established. A case study for validation is presented in Sec. 5. Conclusions are included in the Sec. 6. To ensure the clarity and simplicity, the extensive theory and derivations are provided in the Appendix A.

2 Assumptions and Variation Factors

Without losing generality, we consider the following assembly process: Parts are positioned and assembled sequentially to a root part. Once a nonroot part is joined with the root part, the resulting subassembly will form a new root part. The root part can be identified as a part that is completely kinematically constrained by a fixture. The other parts can be positioned by either part-part mating interface and fixture or both. All parts are completely constrained but without over constraints. To avoid overconstraints, we further assume that the fixture for a nonroot part loses its constraint function once the part is joined and is ignored in subsequent modeling process. Under this assumption, the rigid model actually approximates a natural state of the subassembly. A global coordinate system (GCS) is set up on the root part, and on each part a representative point (RP) is defined. The quality state of current assembly can thus be represented by a vector composed of all the deviations of RPs in the GCS.

We assume all the assembly operations are accomplished in a single station. It implies there is no interstation fixture change that may introduce a datum change and extra deviation by interstation

interaction, until the subassembly leaves the station. The interstation interactions and the complete model for multistation assembly will be discussed in a separate paper.

The variation factors or error sources in the model include part and fixture locating errors. Part errors are defined with respect to a datum, which on a sheet metal panel is assumed to be coincident to part-positioning datum in the assembly process and measured in a local coordinate system (LCS) fixed on the part. Therefore, the datum for a specific part can either be composed of fixture locating points alone (e.g., a root part) or a combination of fixture locating points and part-part mating interfaces. Thus, the datum shift can be caused by these two error sources in upstream assembly processes and change the quality state of the assembly.

Dimensional error and geometric error will be used for tolerance modeling of fixture locators and mating surfaces, respectively. The fixture locator, as a point contact constraint, can be taken as a degenerated mating surface constraint. It is customary in mechanical design to use a simple mating feature to provide stable and secure kinematics joints between parts. Examples include the planar, cylindrical, conical, spherical, and free surfaces, as summarized in Sec. 4.2. For these mating features, the statistical modal analysis (SMA) method [10,27] provides a generic technique for geometric error modeling, which characterizes form errors with superposition of modes. To simplify the modeling process, rigid modes will be composed to represent geometric errors on these mating surfaces. It implies that these modes dominate error patterns and higher deformation modes are trifle.

In summary, the following assumptions are introduced in subsequent modeling process:

1. All parts are completely constrained.
2. There are only fixture locator errors and part mating feature errors; the errors are small and none of the locating points will lose contact.
3. Locator-part constraint is characterized by frictionless point contact.
4. The surface of a part is smooth, with piecewise differentiable regions. The edges and the vertices are not used for fixture locating point. A unique surface normal vector is unambiguously defined at each point.
5. All parts are absolutely rigid.
6. There is no datum change for the root part (valid for single station model).
7. The mating feature geometric error is defined with respect to part datum, which is identical to assembly locating data (e.g., sheet metal part).
8. The geometric errors on the aforementioned features can be simplified by superposition of rigid modes.

Assumptions 1–4 are requirements that must be ensured in the part and fixture design process. Each part needs to be fully constrained by a 3-2-1 scheme (rigid part) and firmly held by clampers. Losing contact is only possible in n-2-1 case with $n>3$, and it can be modeled by a compliant assembly model. Losing contact is equivalent to out-of-plane locator errors; in the open assembly (i.e., not a structural closure with locked-in stresses) case, it has been proven that the effects of these errors can be ignored [9,31]. Rigidness is a widely accepted and applied assumption in variation analysis [1–3,7–9,11–20]; in particular, it is valid for the open assembly. The rigid model will play an important role in the complete assembly model, which characterizes both rigid and compliant components in the open and closing assembly processes. There is no datum change in a single station, i.e., assumption 6 is valid. The part error can be defined and measured with respect to a reference or a datum on it (e.g., a measurement fixture) and the part errors can be formulated in different data systems through simple linear transformations. Assumption 8 has been the basis of dimensional variability parameterization in current tolerancing and variation analysis.

In an assembly process, a root part is initially positioned by a fixture. The mating feature of the root part along with a new fixture provide constraints to a new coming part. By joining these two a new root part (subassembly) is formed. The similar positioning operation repeats until the final subassembly is finished in the assembly station. In a type-I assembly, the mating interface of the root part provides the complete constraints, whereas in a type-II assembly both the root part and the new fixture provide constraints. Therefore, modeling the deviation of a part caused by positioning error in a universal constraining condition is a fundamental step toward the modeling of an assembly process with multiple parts. The 3-2-1 locating scheme in fixture design provides a unified framework for this modeling step, which will be described in Secs. 3 and 4.1. Iteratively conducting this step in light of assembly sequence will eventually establish the assembly model.

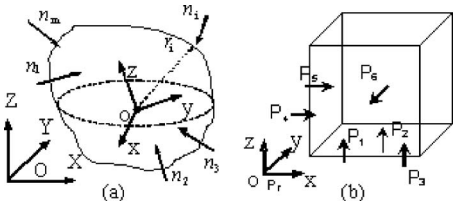

Fig. 1 Examples of kinematics joints: (*a*) generalized fixture layout, (*b*) 3-2-1 fixture scheme

3 Generic Fixture Model

Under the frictionless-point contact assumption, a variation analysis model for a part that is fully constrained by a generalized fixture is established in this section. By generalized fixture, we mean a virtual fixture with the 3-2-1 locating scheme that is equivalent to all kinematics constraints on a part produced by part-part mating interface, fixture, or both. To create equivalent locating points on mating surfaces, rigid modes are assumed and virtual locating points can thus be determined [9].

We start with a generic case as shown in Fig. 1(*a*). A rigid body is constrained by multiple locating (contact) points. At each contact, we assume that a surface normal is known. Two coordinate systems are defined: An LCS oxyz that is fixed on the part and a GCS OXYZ.

Assume there are m locating points, which come from either fixture locators or selected mating feature points. The normal vectors of these points are defined as $\boldsymbol{n}_1,\boldsymbol{n}_2,\ldots,\boldsymbol{n}_m$, and the positions of these locating points are $\boldsymbol{r}_1,\boldsymbol{r}_2,\ldots,\boldsymbol{r}_m$, which are expressed in LCS. To analyze the part deviation caused by fixture errors, in the light of the geometric perturbations analysis [29,32], we assume that the ith locator has a small perturbation $\delta\boldsymbol{r}_i$. For simplicity, let us select a local origin "o" as the part reference point. The resultant part translational and rotational deviation can be expressed as $\delta\boldsymbol{q}=[\delta x\ \ \delta y\ \ \delta z\ \ \delta\alpha\ \ \delta\beta\ \ \delta\gamma]^T$-with respect to the reference point. The relation between locating points error and part deviation can be expressed as

$$\delta\boldsymbol{f}_i = h_i^T\delta q \tag{1}$$

where $\boldsymbol{h}_i^T=-[\boldsymbol{n}_i^T\ \ (\boldsymbol{r}_i\times\boldsymbol{n}_i)^T]$, $\delta\boldsymbol{f}_i=n_i^T\delta\boldsymbol{r}_i\cdot\delta\boldsymbol{f}_i$ is the locating points deviation projected on the contact point's normal direction. For a generalized fixture with m locating points, the equation for whole fixture system is

$$\delta\boldsymbol{f} = \boldsymbol{F}\,\delta\boldsymbol{q} \tag{2}$$

where $\delta\boldsymbol{f}=[\delta\boldsymbol{f}_1,\delta\boldsymbol{f}_2,\ldots,\delta\boldsymbol{f}_m]^T$ and $\boldsymbol{F}=[\boldsymbol{h}_1,\boldsymbol{h}_2,\ldots,\boldsymbol{h}_m]^T$. Matrix $\boldsymbol{F}$ is called the *locator matrix* and completely characterizes the kinematics of the fixture LCS [32]. One of the fundamental requirements for fixture system is deterministic localization, which indicates that the part cannot make an infinitesimal motion without losing contact with at least one locating point [29]. Mathemati-

Table 2 Coordinates for 3-2-1 locators

Locating points	$\boldsymbol{r}_i$	$\boldsymbol{n}_i$
P_1	(x_1,y_1,z_1)	(0,0,1)
P_2	(x_2,y_2,z_2)	(0,0,1)
P_3	(x_3,y_3,z_3)	(0,0,1)
P_4	(x_4,y_4,z_4)	(1,0,0)
P_5	(x_5,y_5,z_5)	(1,0,0)
P_6	(x_6,y_6,z_6)	(0,−1,0)

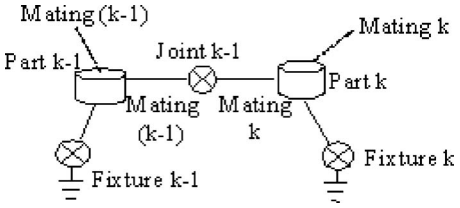

Fig. 2 Assembly chain in a single station

cally, this is true if and only if matrix $\boldsymbol{F}$ is full rank, i.e., rank($\boldsymbol{F}$)=6. That also implies the matrix $\boldsymbol{F}$ is invertible. Let us rewrite Eq. (1) as

$$\delta \boldsymbol{q} = \boldsymbol{F}_s \delta \boldsymbol{y} \tag{3}$$

where $\boldsymbol{F}_s = \boldsymbol{F}^{-1}$. Equation (3) clearly shows how the locating point errors are related to the deviation of part reference point under the condition of rank($\boldsymbol{F}$)=6. The 3-2-1 principle is the most widely used principle for a location scheme. Following this principle, three surfaces are selected to locate a rigid part.

On the first surface—the primary plane, three positions are selected for making locating contact with the part. In a similar way, two positions are selected on the secondary plane, and one on the third surface-tertiary plane. Figure 1(*b*) illustrates the 3-2-1 locating scheme with associated locating points P_1–P_6 (P_6 is on the back face of the object). Here, we apply Eq. (2) to the 3-2-1 fixture scheme and develop the specific $\boldsymbol{F}$ matrix, which will be used to construct an assembly system model in Sec. 4. The position and normal vectors for six locators are listed in Table 2. All coordinates can be expressed in part LCS oxyz.

Let us define a fixture error vector as

$$\Delta f = \boldsymbol{\delta f} = [\Delta z_1 \quad \Delta z_2 \quad \Delta z_3 \quad \Delta x_4 \quad \Delta x_5 \quad \Delta y_6]^T$$

and part reference point $\boldsymbol{P_r}$ at the origin of the part LCS. For any rigid object the variation of it can be characterized by the deviation of any point on it. Denote $\Delta \boldsymbol{P_r}$ as deviation of the part in OXYZ. According to Eq. (3), we have

$$\Delta P_r = \bar{F}_s \Delta f = \Phi F^{-1} \Delta f \tag{4}$$

where $\Phi = \begin{bmatrix} \phi_{3*3} & 0_{3*3} \\ 0_{3*3} & \phi_{3*3} \end{bmatrix}$ $\overline{F_s} = \Phi F^{-1}$ represents the part local-GCS and ϕ (see Appendix A) is

$$\phi = \begin{bmatrix} l^x & m^x & n^x \\ l^y & m^y & n^y \\ l^z & m^z & n^z \end{bmatrix}$$

(l, m, n) represents division number for individual superscripts x, y, and z or axes of oxyz in global system OXYZ. $\Delta \boldsymbol{P_r}$ is the deviation of P_r expressed in GCS.

For a root part, the deviation is caused by fixture alone and can be directly expressed by Eq. (4). In general, the generalized fixture error Δf comes from either a fixture alone or mating interface alone, or both. Therefore, it allows modeling all possible combinations of them for both type-I and type-II assemblies. Δf is usually defined in a LCS, whereas the accumulated variation is normally expressed in product global coordinate. Hence, the coordinate transformation should be carried out before integrating each submodel together.

If Δf includes the deviation components of both true fixture locators and the virtual fixture locators from mating interface, then the impact of Δf on ΔP_r from these two types of locators can be represented in the corresponding columns of $\bar{F}_s$. By partitioning $\bar{F}_s$ accordingly the contributions of these locators can thus be determined in a submatrix conveniently from Eq. (4). The contribution from virtual locators is joint-type specific and will be presented in Sec. 4. Once the contribution models for all the locators are determined, the variation model for a two-part assembly will be established by assembling them in $\bar{F}_s$ accordingly.

4 3D Single-Station Assembly Model

4.1 Modeling Methodology. At system level, an assembly process for a complete product can be expressed by an assembly process graph [9], wherein each single step can be expressed in Fig. 2 as an assembly chain. In this section, we only consider a general operation step involving only two parts in the entire assembly process, which provides an elementary building block for subsequent modeling process.

Assume part $k-1$ is a root part, which can be a single part or a new root part assembled through the upstream $k-1$ steps. It is full constrained by a fixture indexed $k-1$. The deviation model of the root part has been established in Sec. 3, Eq. (4), and its deviation is denoted as $\Delta P_{r(k-1)}$. A new part k is joining this root part in kth step (Fig. 2). Part k is positioned and constrained by the root part (via mating surface on the joining edge) and a fixture. The deviation of part k, denoted as ΔP_{rk}, is caused by the errors of the fixture and the joint between $k-1$ and k. Let us define a reference point (RP) for each part. The contributors to the deviation of part $k\Delta P_{rk}$ are

1. Deviation of the RP on part $k-1$, i.e., $\Delta \boldsymbol{P}_{r(k-1)}$
2. Errors on mating surfaces in joint $k-1$ (between part $k-1$ and part k), i.e., $\Delta\Omega_{(k-1)}$ and $\Delta\Omega_k$
3. Fixture error on part k, i.e., $\Delta \boldsymbol{f}_k$

By applying the lemmas and theorem in Appendix A to the assembly illustrated in Fig. 2, we have

$$\Delta P_{rk} = \bar{J}_{k-1} \begin{Bmatrix} P_{r(k-1)} \\ \Delta\Omega_{(k-1)} \\ \Delta\Omega_k \\ \Delta f_k \end{Bmatrix} = [\bar{J}^j_{k-1} | \bar{J}^f_{k-1}] \begin{Bmatrix} P_{r(k-1)} \\ \Delta\Omega_{(k-1)} \\ \Delta\Omega_k \\ \Delta f_k \end{Bmatrix} \tag{5}$$

where $\bar{J}_{k-1}$ is composed of the submatrices $\bar{J}^f_{k-1}$ and $\bar{J}^j_{k-1}$, which are transformation matrices for the contributions from fixture $\Delta \boldsymbol{f}_k$ and joint $k-1$, respectively. Derivation of the submatrix for the planar joint, which is the commonly used joint in sheet metal assembly, is provided in the Appendix A as well. The key is to translate the mating surface into point contact constraints in the 3-2-1 locating scheme. Typical kinematical joints in mechanical assemblies are summarized in Fig. 3. A control vector based method for the translation is given in Sec. 4.2.

Equation (5) presents the variation propagation between part $k-1$ and part k as illustrated in Fig. 2. Equation (5) is a linear model under the small error assumption, which assures the rotation transformation be linearized, as shown in Eqs. (A1)–(A3) and Lemmas 1-4 in the Appendix A. When multiple parts are assembled in the station following a specified sequence, the variation flow can be expressed by the same formula Eq. (5). There-

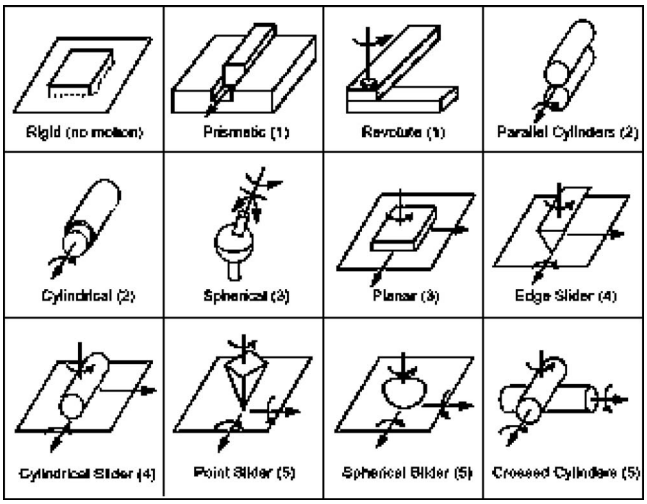

Fig. 3 Examples of kinematics joints

fore, by applying Eq. (5) iteratively for the subsequent joining parts the variation model for the assembly process can be established, which will be presented in Sec. 4.3.

4.2 Unified Joint Model. In an assembly process, parts are positioned by both fixtures and part-to-part joints, or assembly mating features. The geometric errors on these features induce dimensional variation to the assembled product. In this section, an unified joint modeling method is presented. The procedure is given as follows:

1. Create assembly chain for an assembly (Fig. 2) in a single station under study. This chain represents a subgraph of a complete assembly graph for the product.
2. Identify initial root part, operation sequence, kinematical joints, and fixtures for the subassembly.
3. Analyze the constraints by screw theory, generate twist matrix, and wrench matrix.
4. Discretize the mating constraints into control vectors according to the twist matrix.
5. Generate disturbances for control vectors based on the tolerance information.
6. Integrate all the control vectors and use them as inputs to the generalized fixture model developed in Sec. 2.

Table 4 Type of mating joint constraint

Dof constraints	Constraints (15 total)	Joint realization
1	0m1f, 1m0f	Point slider (0m1f) Spherical slider (0m1f) Crossed cylinders (0m1f)
2	0m2f, 1m1f, 2m0f	Cylindrical slider (1m1f) Edge slider (1m1f)
3	0m3f, 1m2f, 2m1f, 3m0f	Spherical (0m3f) Planar (2m1f)
4	1m3f, 2m2f, 3m1f	Cylindrical (2m2f) Parallel cylinders (2m2f)
5	2m3f, 3m2f	Prismatic (3m2f) Revolute (2m3f)
6	3m3f	Rigid mating (3m3f)

Table 3 presents the discretization of mating joints. In Table 3, several typical kinematical joints are described. The twist matrix and wrench matrix for each joint, which lead to degree-of-freedom (DOF) constraints, are provided. In the column of DOF constraints, we use the notation "***imjf***" which means the wrench matrix provides i moment constraints and j force constraints, where $i, j=0-3$. In other words, this wrench matrix represents i rotations and j linear translations constraints. Then, these constraints are expressed by control vectors (virtual locators) in 3-2-1 orthogonal frame, which provide the equivalent number of virtual locators or DOF constraints.

All possible wrench matrices produce 15 types of constraints that can be realized by kinematical joints as shown in Table 4.

Table 3 Discretization of mating joints

Joints	Control vectors	DOF constraints	Twist matrix	Wrench matrix
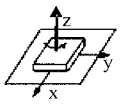	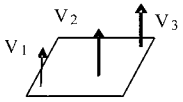	3-0-0 (2m1f)	$\begin{bmatrix}0&0&0&1&0&0\\0&0&0&0&1&0\\0&0&1&0&0&0\end{bmatrix}$	$\begin{bmatrix}0&0&1&0&0&0\\0&0&0&1&0&0\\0&0&0&0&1&0\end{bmatrix}$
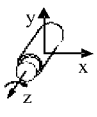	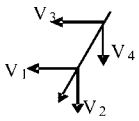	2-2-0 (2m2f)	$\begin{bmatrix}0&0&1&0&0&0\\0&0&0&0&0&1\end{bmatrix}$	$\begin{bmatrix}1&0&0&0&0&0\\0&1&0&0&0&0\\0&0&0&1&0&0\\0&0&0&0&1&0\end{bmatrix}$
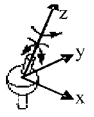	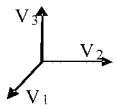	1-1-1 (0m3f)	$\begin{bmatrix}1&0&0&0&0&0\\0&1&0&0&0&0\\0&0&1&0&0&0\end{bmatrix}$	$\begin{bmatrix}1&0&0&0&0&0\\0&1&0&0&0&0\\0&0&1&0&0&0\end{bmatrix}$
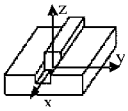	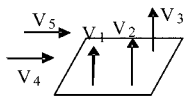	3-2-0 (3m2f)	$\begin{bmatrix}0&0&0&1&0&0\end{bmatrix}$	$\begin{bmatrix}0&1&0&0&0&0\\0&0&1&0&0&0\\0&0&0&1&0&0\\0&0&0&0&1&0\\0&0&0&0&0&1\end{bmatrix}$
⋮	⋮	⋮	⋮	⋮

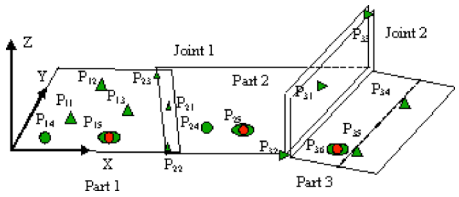

Fig. 4 Case study for validation

Figure 1 presents physical realizations of these constraints in kinematical joints.

4.3 3D Single-Station SOVA Model for Rigid Part. If $N>1$, then parts are sequentially assembled in an assembly station. Assume fixture errors and mating feature errors are the dominant factors to the deviation of the assembly. Following assembly sequence and by applying Eq. (5) iteratively, the deviation of all parts in the assembly, denoted by $\{\Delta P_r\}$, can be expressed by:

$$\{\Delta \boldsymbol{P}_r\}_{6N^*1} = \boldsymbol{\Lambda} \cdot \{\bar{\boldsymbol{\Delta}}\}_{m^*1} \tag{6}$$

$$\boldsymbol{\Lambda} = [(\bar{J}_0 \bar{W}_0)^{\mathrm{T}}, (\bar{J}_1 \bar{W}_1)^{\mathrm{T}}, (\bar{J}_2 \bar{W}_2)^{\mathrm{T}}, \ldots, (\bar{J}_{N-1} \bar{W}_{N-1})^{\mathrm{T}}]^{\mathrm{T}} \tag{7}$$

where $\{\Delta \boldsymbol{P}_r\}_{6N^*1} = \{\Delta \boldsymbol{P}'_{r1}, \Delta \boldsymbol{P}'_{r2}, \ldots \Delta \boldsymbol{P}'_{rN}\}'$

$$\bar{\boldsymbol{W}}_0 = [\bar{F}_s | 0, \ldots, 0]_{6^*m}, \quad m = 15N - 3, \quad \bar{J}_0 = I_{6\times 6}$$

$$\bar{W}_1 = \begin{bmatrix} \bar{W}_0 \\ U_0 \end{bmatrix}_{21\times m}, \quad U_0 = [0_{15\times 6} | I_{15\times 15} | 0 \ldots 0]_{15\times m}$$

$$\bar{W}_2 = \begin{bmatrix} \bar{J}_j \bar{W}_j \\ U_1 \end{bmatrix}_{21\times m}, \quad U_1 = [0_{15\times(6+15)} | I_{15\times 15} | 0 \ldots 0]_{15\times m},$$

$$j = 0, \ldots, 1$$

$$\bar{W}_3 = \begin{bmatrix} \bar{J}_j \bar{W}_j \\ U_2 \end{bmatrix}_{21\times m}, \quad U_2 = [0_{15^*(6+2\times 15)} | I_{15^*15} | 0 \ldots 0]_{15\times m},$$

$$j = 0, \ldots, 2$$

$$\vdots$$

$$\bar{W}_k = \begin{bmatrix} \bar{J}_j \bar{W}_j \\ U_{k-1} \end{bmatrix}_{21\times m}, \quad U_{k-1} = [0_{15^*[6+(k-1)^*15]} | I_{15^*15} | 0 \ldots 0]_{15\times m},$$

$$j = 0, \ldots, k-1$$

where $\Delta \boldsymbol{f}_1$ is 6 by 1 vector, and $\Delta \boldsymbol{f}_k (k=2-N)$ is 3 by 1 vector. $\bar{\boldsymbol{J}}_1, \ldots, \bar{\boldsymbol{J}}_{N-1}$ are defined in Eq. (5).

Proof. From Eq. (4), the root part deviation is

$$\Delta \boldsymbol{P}_{r1} - \bar{\boldsymbol{F}}_s \cdot \Delta f_1 = \bar{\boldsymbol{W}}_0 \bar{\Delta}$$

Applying Eq. (4) to part k, $\{k=2,3,\ldots,N\}$,

$$\{\bar{\Delta}\}' = \{\overbrace{\Delta f'_1, \Delta\Omega'_{12}}^{\text{part I}}, \overbrace{\Delta\Omega'_{21}, \Delta f'_2, \Delta\Omega'_{23}}^{\text{part II}}, \overbrace{\Delta\Omega'_{32}, \Delta f'_2, \Delta\Omega'_{34}}^{\text{part III}}, \overbrace{\ldots, \ldots}^{\ldots}\}_{1^*m}$$

represents all error sources

$$\Delta P_{r2} = \bar{J}_1 \begin{Bmatrix} \Delta P_{r1} \\ \Delta\Omega_{12} \\ \Delta\Omega_{21} \\ \Delta f_2 \end{Bmatrix} = \bar{J}_1 \begin{bmatrix} \bar{F}_0 | 0 \ldots & 0 \\ 0_{15\times 6} & I_{15\times 15} | 0 \ldots 0 \end{bmatrix}_{21\times m} \bar{\Delta}$$

$$= [\bar{J}_1 \bar{W}_1]_{6\times m} \bar{\Delta}$$

$$\Delta P_{r3} = \bar{J}_2 \begin{Bmatrix} \Delta P_{r2} \\ \Delta\Omega_{23} \\ \Delta\Omega_{32} \\ \Delta f_3 \end{Bmatrix} = \bar{J}_2 \begin{bmatrix} \bar{J}_1 \bar{W}_1 \\ 0_{15\times 6(6+15)} | I_{15^*15} | 0 \ldots 0 \end{bmatrix}_{21\times m} \bar{\Delta}$$

$$= [\bar{J}_2 \bar{W}_2]_{6\times m} \bar{\Delta}$$

$$\vdots$$

and

$$\{\Delta \mathrm{P}_r\}_{6\mathrm{N}\times 1} = [\bar{W}_0^T, (\bar{J}_1 \bar{W}_1)^T, (\bar{J}_2 \bar{W}_2)^T, \ldots, (\bar{J}_{N-1} \bar{W}_{N-1})^T]^T \cdot \{\bar{\Delta}\}$$

$$= \Lambda \cdot \{\bar{\Delta}\} \tag{8}$$

Corollary 1. *If the fixture/part mating feature errors are multivariate normal, i.e.,* $\bar{\boldsymbol{\Delta}} \sim \mathbf{N}(\bar{\boldsymbol{\mu}}_{\boldsymbol{\Delta}}, \boldsymbol{\Sigma})$, *then*

$$\{\Delta \boldsymbol{P}_r\} \sim N(\boldsymbol{\Lambda}\bar{\boldsymbol{\mu}}_{\Delta}, \boldsymbol{\Lambda}'\boldsymbol{\Sigma}\boldsymbol{\Lambda}) \tag{9}$$

Proof. Equation (9) is obvious by taking expectation and variance operations on both sides of Eq. (8). Equation (9) provides an easy way for statistical variation analysis.

5 Model Validations

Two methods were used to validate the model through simulations: (i) MC simulation without linear approximation in the assembly model and (ii) 3DCS (Dimensional Control Systems Inc. Troy, MI) software-based simulation. The simulation results are compared to that from the developed model-based method in Eqs. (6)–(9).

A case study was designed for the validation as shown in Fig. 4. This assembly combines two types of joints, i.e., butt and lap joints. The linear deviation error input (tolerance) for the model is 2 mm, and the angular deviation is 2.5 deg.

5.1 Model Parameters. An absolute coordinate system and the points used in the model for the case study are illustrated in Fig. 4. These points include fixture locator points, virtual points to represent assembly mating feature positions and orientations. The error sources are the fixture locator errors for three fixtures and the mating feature errors for joints 1 and 2. The fixture errors and mating feature errors (translational) are assumed to follow a normal distribution N (0, 1/3). We did not directly assign tolerance to the virtual locating points on joint mating plane, such as $P_{21}-P_{23}$

Table 5 Coordinates of fixture locators (PLPs) (in centimeters)

P_{11}	P_{12}	P_{13}	P_{14}	P_{15}
(10,15)	(15,25)	(30,10)	(5,5)	(25,5)
P_{24}	P_{25}	P_{34}	P_{35}	P_{36}
(45,10)	(55,15.8)	(90,40)	(82,10)	(70,20)

Table 6 Virtual points on mating feature planes (in centimeters)

P_{21}	P_{22}	P_{23}	P_{31}	P_{32}	P_{33}
(35,15)	(40,0)	(25,30)	(65,30.2,5)	(60,11.5,)	(80,86.1,10)

Table 7 Coordinates of reference points (in centimeters)

P_{r1}	P_{r2}	P_{r3}
(5,5)	(45,10)	(90,40)

Table 8 Reference points deviation predicated by SOVA model (in millimeters per rad)

	Δx	Δy	Δz	$\Delta\alpha$	$\Delta\beta$	$\Delta\gamma$
P_{r_1}	0.3333	0.3333	0.74536	0.003777	0.002772	0.002357
P_{r_2}	0.3333	0.3333	1.4059	0.010956	0.010651	0.004083
P_{r_3}	1.9164	2.0933	0.3333	0.004082	0.014223	0.011065

Table 10 Reference points deviation predicated by 3DCS (in millimeters per rad)

	Δx	Δy	Δz	$\Delta\alpha$	$\Delta\beta$	$\Delta\gamma$
P_{r_1}	0.3329	0.3380	0.7548	0.003797	0.002797	0.002382
P_{r_2}	0.3346	0.3351	1.4097	0.010834	0.010722	0.004101
P_{r_3}	1.9222	2.0681	0.3356	0.004093	0.014144	0.011039

and $P_{31}-P_{33}$. They can be obtained from the tolerances assigned on these features [9]. Angular errors of these features are assumed following $N(0,(2.5\pi/180)/6)$, i.e., ($\pm$1.25 deg). For simplicity, all data points are in the $Z=0$ plane. There are two mating feature planes: the first one is lap joint with 30 deg rotation with respect to z-axis, and the second one is a butt joint with -15 deg rotation about z-axis.

All the coordinates of locator and feature points are given in Tables 5–7.

5.2 Validation Results. The model output of Eqs. (6) and (9) is the variation of the reference point for each part in the assembly. These results were compared to the simulation results by using the MC and 3DCS model.

5.2.1 Validation with Monte Carlo Simulation. The MC simulation is based on the complete model without any linear approximation and the run number is set to 10,000. The results showed that the differences (relative errors) between the developed SOVA model and MC simulation are $<2\%$. The results of the SOVA model are shown in Table 8, and the MC Simulation results are shown in Table 9. The relative errors are defined as $100\% * |\sigma_{MC}-\sigma_{SOVA}|\sigma_{MC}$ are shown in Fig. 5(*a*).

In addition, the computation effort involved in the analysis also justified the advantage of the SOVA model over MC-based simulation. The ratio of computation efforts in terms of the time spent in calculations is 0.328% (0.02 s for SOVA model versus 60.97 s for MC). Most of the time was consumed on the large number of model calculations. The computational intensity is a critical issue in large-scale system design analysis. For example, in tolerance synthesis, the variation analysis will be embedded in optimization inner loops for iterative optimal point searching. Industrial cases usually involve thousands of design variables and thus can produce prohibitive computational difficulties in simulation based methods.

Table 9 Reference points deviation predicated by MC simulation (in millimeters per rad)

	Δx	Δy	Δz	$\Delta\alpha$	$\Delta\beta$	$\Delta\gamma$
P_{r_1}	0.3325	0.3272	0.7370	0.003763	0.002750	0.002326
P_{r_2}	0.3363	0.3312	1.4189	0.011044	0.010575	0.004071
P_{r_3}	1.9112	2.0937	0.3320	0.004139	0.014406	0.011056

5.2.2 Validation With 3DCS ANALYST Simulation. 3DCS ANALYST is used as a benchmark for the validation. 3DCS ANALYST is a prevailed industrial dimensional variation simulation software. By building the point-based model according the case shown in Fig. 4, we simulated the dimensional variation in 3DCS ANALYST. The run number is set to 5000.

The results of 3DCS ANALYST and MC simulation are compared to those of the SOVA model. The comparisons are shown in Tables 8–10. Figure 5(*b*) shows the percentage differences (relative error) between the 3DCS ANALYST and SOVA models. The percentage difference is $<1.5\%$.

6 Conclusions and Future Work

A SOVA model for 3D rigid-body assemblies in a single assembly station is developed and validated in this paper. The model takes into account various part-to-part and part-to-fixture interactions through a *generalized virtual fixture* model. Both type-I and type-II assemblies with a variety of mating joints can be formulated in a unified framework. This is an initial step toward the goal of developing a generic 3D assembly model for multistation manufacturing processes.

The latest advances in 3D rigid-body SOVA model for multistation assembly processes and their applications in variation control can be found in [22,23].

The advantages of the developed model over traditional MC based simulation include: (i) better computational efficiency, which is critical for applications in large scale complex manufacturing systems [23], in particular, for backward application in synthesis and diagnosis; (ii) it provides the basis for a generic 3D rigid assembly model for stream of variation in multistation systems [22]; and (iii) it allows both tolerance analysis and tolerance synthesis through an explicit input-output model [23].

The potential applications of the SOVA model include both forward and backward applications (analysis and synthesis or di-

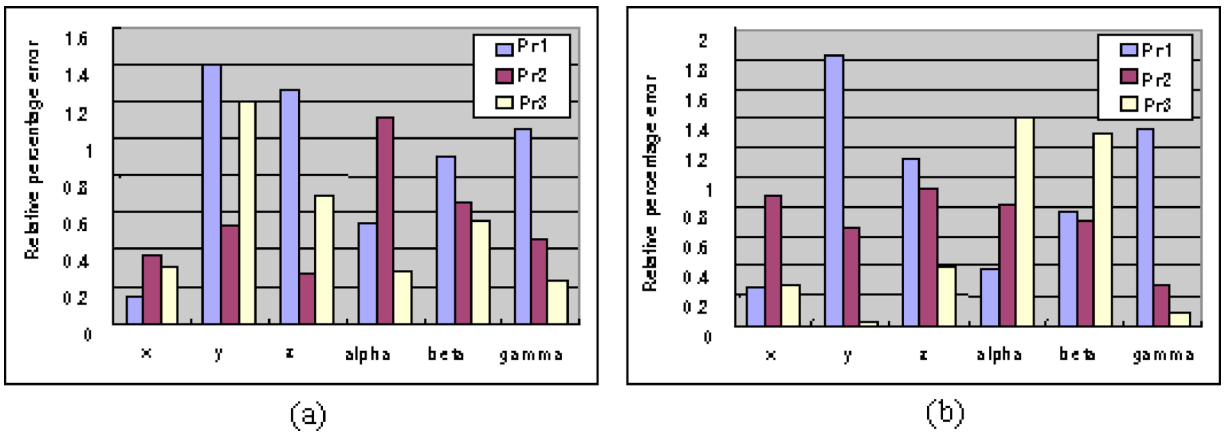

Fig. 5 (*a*) Relative errors of SOVA versus MC and (*b*) relative error of SOVA model versus 3DCS

agnosis) for dimensional variation control of complex assemblies in industries, such as automotive, aerospace, shipbuilding, etc. In the forward application, the model allows for variation prediction, tolerance analysis, and sensitivity analysis in design evaluation. For instance, various sensitivity indices, which provide useful information about the most significant contributors, can be defined and assessed for design improvement. In the backward application, the SOVA model can avoid prohibitive numerical computation in current MC-based techniques and thus permits highly efficient tolerance synthesis and fixture layout optimization. It can also provide a powerful tool for dimensional quality faults diagnosis. By incorporating the observation equation into the variation propagation model, a data-model-driven technique can thus be developed, which can take full advantage of fault information in the data and causality in the model.

Acknowledgment

The authors gratefully acknowledge the financial support of the Advanced Technology Program (ATP) Award provided by National Institute of Standards and Technology (NIST). The authors would also like to thank Dimensional Control Systems, Inc, for its enthusiastic support and insightful discussions.NIST

Appendix A

A.1 Lemmas and Theorem

The results used to derive Eq. (6) are presented in the following lemmas and theorem. A typical case in which we are interested is where a rigid part deviates from its nominal position by small translational and rotational movement. We denote this deviation by a 6-tuple $\{\Delta x, \Delta y, \Delta z, \Delta\alpha, \Delta\beta, \Delta\gamma\}$, which is defined on a reference point (RP) P_r. We set a LCS on a selected RP, and the deviation of the part is represented by ΔP_r. The 6-tuple also represents a set of transformations. Lemma 1 shows the operational commutativity of the set of transformations under small deviation assumption. Thus, the sequence of the transformations can be ignored. The transformation between deviations of any two points on a part are summarized in Lemmas 2 and 3. Lemma 4 provides a easy way for concatenating transformations.

The 6-tuple is equivalent to a set of translational and rotational transformations. Under small error assumption, the transformation matrices for counterclockwise rotations about z-, y-, and x-axes can be approximately expressed as

$$R_1 = \begin{bmatrix} \cos\Delta\gamma & -\sin\Delta\gamma & 0 & 0 \\ \sin\Delta\gamma & \cos\Delta\gamma & 0 & 0 \\ 0 & 0 & 1 & 0 \\ 0 & 0 & 0 & 1 \end{bmatrix} = \begin{bmatrix} 1 & -\Delta\gamma & 0 & 0 \\ \Delta\gamma & 1 & 0 & 0 \\ 0 & 0 & 1 & 0 \\ 0 & 0 & 0 & 1 \end{bmatrix} \tag{A1}$$

$$R_2 = \begin{bmatrix} \cos\Delta\beta & 0 & -\sin\Delta\beta & 0 \\ 0 & 1 & 0 & 0 \\ \sin\Delta\beta & 0 & \cos\Delta\beta & 0 \\ 0 & 0 & 0 & 1 \end{bmatrix} = \begin{bmatrix} 1 & 0 & \Delta\beta & 0 \\ 0 & 1 & 0 & 0 \\ -\Delta\beta & 0 & 1 & 0 \\ 0 & 0 & 0 & 1 \end{bmatrix} \tag{A2}$$

$$R_3 = \begin{bmatrix} 1 & 0 & 0 & 0 \\ 0 & \cos\Delta\alpha & -\sin\Delta\alpha & 0 \\ 0 & \sin\Delta\alpha & \cos\Delta\alpha & 0 \\ 0 & 0 & 0 & 1 \end{bmatrix} = \begin{bmatrix} 1 & 0 & 0 & 0 \\ 0 & 1 & -\Delta\alpha & 0 \\ 0 & \Delta\alpha & 1 & 0 \\ 0 & 0 & 0 & 1 \end{bmatrix} \tag{A3}$$

The translation matrix is

$$M = \begin{bmatrix} I_{3*3} & \Delta \\ 0 & 1 \end{bmatrix}, \quad \Delta = [\Delta x, \Delta y, \Delta z]^{\mathrm{T}} \tag{A4}$$

Let us denote the transformation as $T=[R_3R_2R_1M]$. The reverse transform T^{-1} is defined as a transformation from $\{\Delta x, \Delta y, \Delta z, \Delta\alpha, \Delta\beta, \Delta\gamma\}$ to $\{0,0,0,0,0,0\}'$. It is easy to show that the reverse transform $T^{-1}(\Delta x, \Delta y, \Delta z, \Delta\alpha, \Delta\beta, \Delta\gamma) = T(-\Delta x, -\Delta y, -\Delta z, -\Delta\alpha, -\Delta\beta, -\Delta\gamma)$. The translations are commutative; a set of translations can be multiplied or concatenated together to give a net matrix.

Lemma 1. *Transformations for rotation and translation are approximately commutative under small deviation assumption, i.e.*,

$$R_iR_j \approx R_jR_i, \quad M_iM_j \approx M_jM_i, \quad \text{and} \quad M_iR_j \approx R_iM_j$$

Proof. Lemma 1 *can be proved by using matrix manipulation and ignoring higher-order terms* $[O(\Delta^2)]$. QED.

Lemma 2. *When a rigid body undergoes translations and rotations away from its nominal position, if the rotation angles* (*denoted as* $(\Delta\alpha, \Delta\beta, \Delta\gamma)$) *is small, then deviations of any given point* $P(x,y,z)$ (*denoted as* $\Delta P = \{\Delta x, \Delta y, \Delta z, \Delta\alpha, \Delta\beta, \Delta\gamma\}^T$) *and a RP* P_r (0, 0, 0) (*denoted as* $\Delta P_r = \{\Delta x, \Delta y, \Delta z, \Delta\alpha, \Delta\beta, \Delta\gamma\}_r^T$) *on that part have the following relationship*:

$$\{\Delta P\} = \begin{bmatrix} I & Q \\ 0 & I \end{bmatrix} \cdot \{\Delta P_r\} = \bar{Q} \cdot \{\Delta P_r\}, \tag{A5}$$

$$Q = \begin{bmatrix} 0 & z & -y \\ -z & 0 & x \\ y & -x & 0 \end{bmatrix}$$

Proof. From Lemma 1 and (A1)–(A4), through matrices manipulations and truncating the higher-order terms Eq. (A5) can be proved [14]. Equation (A5) represents the relationship between deviation $\{\Delta P_r\}$ of a RP and the deviation $\{\Delta P\}$ of any point $P(x,y,z)$ on the part. QED

Lemma 3. *If the deviation at point* $P_i(x_i, y_i, z_i)$ *is known* $\Delta P_i = \{\Delta x, \Delta y, \Delta z, \Delta\alpha, \Delta\beta, \Delta\gamma\}_i'$, *then the deviation of any other point* $P_k(x_k, y_k, z_k)$ *on the same part, denoted as* $\Delta P_k = \{\Delta x, \Delta y, \Delta z, \Delta\alpha, \Delta\beta, \Delta\gamma\}_k'$ *can be expressed as*

$$\Delta P_k = \begin{bmatrix} I & Q_k - Q_i \\ 0 & I \end{bmatrix} \Delta P_i = \bar{Q}_{ik} \Delta P_i \tag{A6}$$

Proof. Note that $\begin{bmatrix} I & Q_i \\ 0 & I \end{bmatrix}^{-1} = \begin{bmatrix} I & -Q_i \\ 0 & I \end{bmatrix}$, it is easy to show Eq. (A6) holds. QED.

Lemma 4. *When a point on a rigid body undergoing a series of small transformation, these sequential transformations under linear approximation can be expressed as*

$$\prod_{i=1}^{n} T_i(\Delta_i) = T\left(\sum_{i=1}^{n} \Delta_i\right), \qquad n \geq 2 \tag{A7}$$

where the transformation $T(\Delta)$ is defined in Eqs. (A1)–(A4)

$$T(\Delta)=T(\Delta x,\Delta y,\Delta z,\Delta\alpha,\Delta\beta,\Delta\gamma)=[R_3R_2R_1M] \text{ or}$$

$$T_i(\Delta_i)=\begin{bmatrix} 1 & -\Delta\gamma_i & \Delta\beta_i & \Delta x_i \\ \Delta\gamma_i & 1 & -\Delta\alpha_i & \Delta y_i \\ -\Delta\beta_i & \Delta\alpha_i & 1 & \Delta z_i \\ 0 & 0 & 0 & 1 \end{bmatrix}$$

$$T(\Sigma)=T(\Sigma\Delta x,\Sigma\Delta y,\Sigma\Delta z,\Sigma\Delta\alpha,\Sigma\Delta\beta,\Sigma\Delta\gamma)$$

$$=\begin{bmatrix} 1 & -\sum_{i=1}^{N}\Delta\gamma_i & \sum_{i=1}^{N}\Delta\beta_i & \sum_{i=1}^{N}\Delta x_i \\ \sum_{i=1}^{N}\Delta\gamma_i & 1 & -\sum_{i=1}^{N}\Delta\alpha_i & \sum_{i=1}^{N}\Delta y_i \\ -\sum_{i=1}^{N}\Delta\beta_i & \sum_{i=1}^{N}\Delta\alpha_i & 1 & \sum_{i=1}^{N}\Delta z_i \\ 0 & 0 & 0 & 1 \end{bmatrix}$$

Proof. (i) We first prove: Lemma 4 holds for $n=2$. By multiplying T_1 and T_2, and deleting higher-order terms, it yields

$$\prod_{i=1}^{2}T_i=T_1T_2\approx\begin{bmatrix} 1 & -\sum_{i=1}^{2}\Delta\gamma_i & \sum_{i=1}^{2}\Delta\beta_i & \sum_{i=1}^{2}\Delta x_i \\ \sum_{i=1}^{2}\Delta\gamma_i & 1 & -\sum_{i=1}^{2}\Delta\alpha_i & \sum_{i=1}^{2}\Delta y_i \\ -\sum_{i=1}^{2}\Delta\beta_i & \sum_{i=1}^{2}\Delta\alpha_i & 1 & \sum_{i=1}^{2}\Delta z_i \\ 0 & 0 & 0 & 1 \end{bmatrix}$$

$$=T\left(\sum_{i=1}^{2}\Delta_i\right)$$

(ii) Assume Lemma 4 holds for $k=m$. In a similar way, it is easy to show that Lemma 4 also holds for $k=m+1$

$$\prod_{i=1}^{m+1}T_i(\Delta_i)=\left[\prod_{i=1}^{m}T_i(\Delta_i)\right]T_{m+1}$$

$$\approx\begin{bmatrix} 1 & -\sum_{i=1}^{m+1}\Delta\gamma_i & \sum_{i=1}^{m+1}\Delta\beta_i & \sum_{i=1}^{m+1}\Delta x_i \\ \sum_{i=1}^{m+1}\Delta\gamma_i & 1 & -\sum_{i=1}^{m+1}\Delta\alpha_i & \sum_{i=1}^{m+1}\Delta y_i \\ -\sum_{i=1}^{m+1}\Delta\beta_i & \sum_{i=1}^{m+1}\Delta\alpha_i & 1 & \sum_{i=1}^{m+1}\Delta z_i \\ 0 & 0 & 0 & 1 \end{bmatrix}$$

$$=T\left(\sum_{i=1}^{m+1}\Delta_i\right)$$

by deduction the conclusion holds for all n. QED

Theorem 1. *The deviation of a RP on part k can be determined by*

1. *The deviation of the RP on part k-1, i.e.,* $\Delta P_{r(k-1)}$
2. *The errors of joint k-1, i.e.,* $\Delta\Omega_{b(k-1)}$ *and* $\Delta\Omega_{ak}$
3. *Fixture error on part k, i.e.,* Δf_k, *i.e.,*

$$\Delta P_{rk}=\bar{J}_{k-1}\cdot\{\Delta P_{r(k-1)},\Delta\Omega_{b(k-1)},\Delta\Omega_{ak},\Delta f_k\}^T \quad \text{(A8)}$$

Proof. Using Lemma 2 to RP $P_{r(k-1)}$, the deviation of point $P_{\Omega b}$ can be obtained. Denote the 6-tuples $\Delta P_{\Omega b(k-1)}$, $\Delta\Omega_{b(k-1)}$, $\Delta\Omega_{ak}$ as T_1, T_2, T_3, then the deviations accumulated from part $k-1$ through joint $k-1$ can be calculated by concatenating using Lemma 4. Using these results with the contribution of fixture k errors on the deviation of reference point P_{rk} Theorem 1 can be proved. The detailed process to construct these transformation matrices in $\bar{J}_i$ will be presented in Sec. A.3. QED

Eq. (A8) will be utilized to construct the complete variation propagation model for a single assembling station.

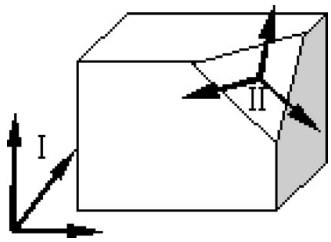

Fig. 6 Mating feature plane at arbitrary position and orientation

A.2 Coordinate System Transformation

To account for mating feature with arbitrary position and orientation (Fig. 6), we introduce a transformation to represent the deviation in different GCSs.

a Rotation Representation by Unit Vector. Assume that there are two GCSs A and B, The GCS B is fixed on the ground and initially aligned with the GCS A. GCS A is fixed on the rigid body and rotates with it. This rotation can be expressed as an axis vector $\vec{m}$ with direction number of $\{m_x,m_y,m_z\}$ and rotation angle θ about $\vec{m}$. $\vec{m}$ passes the origin (Fig. 7). By introducing a coordinate system C whose z-axis is parallel to $\vec{m}$, the rotation transformation denoted as ${}^A_BR$ can be obtained [33]:

$${}^A_BR=\begin{bmatrix} m_xm_xv+c & m_xm_yv-m_zs & m_xm_zv+m_ys \\ m_xm_yv+m_zs & m_ym_yv+c & m_ym_zv-m_xs \\ m_xm_zv-m_ys & m_ym_zv+m_xs & m_zm_zv+c \end{bmatrix} \quad \text{(A9)}$$

Here, $v=(1-\cos\theta)$, $c=\cos\theta$, $s=\sin\theta$. Since it is a small rotation or $\theta\ll1$, so $v\approx0$, $c\approx1$, $s\approx\theta$. A rotation can also be approximately expressed as

$${}^A_BR=\begin{bmatrix} 1 & -\Delta\gamma & \Delta\beta \\ \Delta\gamma & 1 & -\Delta\alpha \\ -\Delta\beta & \Delta\alpha & 1 \end{bmatrix}$$

By comparison, it yields

$$\theta=\sqrt{(\Delta\alpha)^2+(\Delta\beta)^2+(\Delta\gamma)^2}$$

$$m_x=\frac{\Delta\alpha}{\sqrt{(\Delta\alpha)^2+(\Delta\beta)^2+(\Delta\gamma)^2}}$$

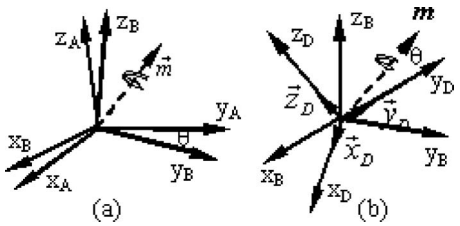

Fig. 7 (*a*) Rotation as a vector and (*b*) rotation in coordinate systems B and D

$$m_y = \frac{\Delta\beta}{\sqrt{(\Delta\alpha)^2 + (\Delta\beta)^2 + (\Delta\gamma)^2}}$$

$$m_z = \frac{\Delta\gamma}{\sqrt{(\Delta\alpha)^2 + (\Delta\beta)^2 + (\Delta\gamma)^2}}$$

Vector $\vec{m}$ with rotation θ represents the rigid-body rotation $\{\Delta\alpha, \Delta\beta, \Delta\gamma\}$ in B.

b Rotation Expression in Different GCS. Assume we have another GCS D whose axis can be expressed in GCS B with unit vectors and their direction numbers $\vec{x}_D$:$\{l^x, m^x, n^x\}$ for x-axis, $\vec{y}_D$:$\{l^y, m^y, n^y\}$ for y-axis, and $\vec{z}_y$:$\{l^z, m^z, n^z\}$ for z-axis, respectively (Fig. 7(*b*)).

To express the angle of vector $\vec{m}$ in GCS D, we can project axis vector $\vec{m}$ into each axis of D. So the direction numbers of $\vec{m}$ in D are: $\{\cos\phi_{\mathrm{mx}}, \cos\phi_{\mathrm{my}}, \cos\phi_{\mathrm{mz}}\}$, where

$$\begin{aligned}
\cos\phi_{mx} &= \vec{x}_D \bullet \mathbf{m} = \vec{m}_x \cdot l^x + m_y \cdot m^x + m_z \cdot n^x \\
\cos\phi_{my} &= \vec{y}_D \bullet \mathbf{m} = \vec{m}_x \cdot l^y + m_y \cdot m^y + m_z \cdot n^y \\
\cos\phi_{mz} &= \vec{z}_D \bullet \mathbf{m} = \vec{m}_x \cdot l^z + m_y \cdot m^z + m_z \cdot n^z
\end{aligned} \tag{A10}$$

Thus, the rotations in GCS D are:

$$\begin{aligned}
\Delta\alpha_D &= \theta\cos\phi_{mx} = \Delta\alpha l^x + \Delta\beta m^x + \Delta\gamma n^x \\
\Delta\beta_D &= \theta\cos\phi_{my} = \Delta\alpha l^y + \Delta\beta m^y + \Delta\gamma n^y \\
\Delta\gamma_D &= \theta\cos\phi_{mz} = \Delta\alpha l^z + \Delta\beta m^z + \Delta\gamma n^z
\end{aligned}$$

$$\text{or} \begin{Bmatrix} \Delta\alpha_D \\ \Delta\beta_D \\ \Delta\gamma_D \end{Bmatrix} = \begin{bmatrix} l^x & m^x & n^x \\ l^y & m^y & n^y \\ l^z & m^z & n^z \end{bmatrix} \begin{Bmatrix} \Delta\alpha \\ \Delta\beta \\ \Delta\gamma \end{Bmatrix} = \Phi \begin{Bmatrix} \Delta\alpha \\ \Delta\beta \\ \Delta\gamma \end{Bmatrix} \tag{A11}$$

Similarly, we can define the translational deviation vector $\vec{\lambda} = \{\Delta x, \Delta y, \Delta z\}$, By projection, we have

$$\begin{Bmatrix} \Delta x_D \\ \Delta y_D \\ \Delta z_D \end{Bmatrix} = \begin{bmatrix} l^x & m^x & n^x \\ l^y & m^y & n^y \\ l^z & m^z & n^z \end{bmatrix} \begin{Bmatrix} \Delta x \\ \Delta y \\ \Delta z \end{Bmatrix} = \Phi \begin{Bmatrix} \Delta x \\ \Delta y \\ \Delta z \end{Bmatrix}$$

It yields $\Delta_D = \bar{\Phi}\Delta$, where $\Delta_D = \{\Delta x, \Delta y, \Delta z, \Delta\alpha, \Delta\beta, \Delta\gamma\}'_D$, $\Delta = \{\Delta x, \Delta y, \Delta z, \Delta\alpha, \Delta\beta, \Delta\gamma\}'$, and

$$\bar{\Phi} = \begin{bmatrix} \Phi_{3*3} & [0]_{3*3} \\ [0]_{3*3} & \Phi_{3*3} \end{bmatrix}$$

A.3 Variation Propagation Through a Joint

Without loss generality, we illustrate an example below with mating plane features. A similar approach can be also applied to more general joints with different mating features. Assume we have an absolute GCS $\boldsymbol{A}$ and a GCS $\boldsymbol{B}$ at a mating feature plane aligned with $\boldsymbol{A}$ and with origin O_Ω. We set another GCS $\boldsymbol{B'}$ aligned with the feature plane but with the same origin O_Ω. A small deviation Δ of a rigid body can thus be transformed between GCSs $\boldsymbol{A}$, $\boldsymbol{B}$, and $\boldsymbol{B'}$ by using $\bar{Q}$ and $\bar{\Phi}$.

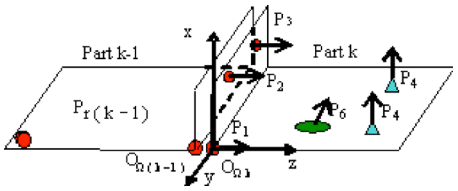

Fig. 8 Point definition at mating planes

In a joint, two mating planes contact and the points $\mathrm{O}_{\Omega(k-1)}$ and $\mathrm{O}_{\Omega k}$ coincide (Fig. 8). Denote the geometric error of the feature planes with $\Delta\Omega_l = (\Delta x_{\Omega_l}, \Delta y_{\Omega_l}, \Delta z_{\Omega_l}, \Delta\alpha_{\Omega_l}, \Delta\beta_{\Omega_l}, \Delta\gamma_{\Omega_l})$, $l = k-1$, and k.

In GCS $\boldsymbol{B'}$ if all the six relative degrees of freedom are constrained by the mating plane, we have the following relations for the complete constraining joint:

$$\begin{aligned}
\Delta x_{O_{\Omega k}} &= \sum \Delta x = \Delta x_{O_{\Omega(k-1)}} + \Delta x_{\Omega(k-1)} - \Delta x_{\Omega k} \\
\Delta y_{O_{\Omega k}} &= \sum \Delta y = \Delta y_{O_{\Omega(k-1)}} + \Delta y_{\Omega(k-1)} - \Delta y_{\Omega k} \\
\Delta z_{O_{\Omega k}} &= \sum \Delta z = \Delta z_{O_{\Omega(k-1)}} + \Delta z_{\Omega(k-1)} - \Delta z_{\Omega k} \\
\Delta\alpha_{O_{\Omega k}} &= \sum \Delta\alpha = \Delta\alpha_{O_{\Omega(k-1)}} + \Delta\alpha_{\Omega(k-1)} - \Delta\alpha_{\Omega k} \\
\Delta\beta_{O_{\Omega k}} &= \sum \Delta\beta = \Delta\beta_{O_{\Omega(k-1)}} + \Delta\beta_{\Omega(k-1)} - \Delta\beta_{\Omega k} \\
\Delta\gamma_{O_{\Omega k}} &= \sum \Delta\gamma = \Delta\gamma_{O_{\Omega(k-1)}} + \Delta\gamma_{\Omega(k-1)} - \Delta\gamma_{\Omega k}
\end{aligned} \tag{A12}$$

In general, the mating feature only constrains less than six degrees of freedom. For the most commonly used mating plane joints in sheet metal assemblies, the following reduced equations can be used:

$$\begin{cases}
\Delta z_{O_{\Omega k}} = \Delta z_{O_{\Omega(k-1)}} + \Delta z_{\Omega(k-1)} - \Delta z_{\Omega k} \\
\Delta\alpha_{O_{\Omega k}} = \Delta\alpha_{O_{\Omega(k-1)}} + \Delta\alpha_{\Omega(k-1)} - \Delta\alpha_{\Omega k} \\
\Delta\beta_{O_{\Omega k}} = \Delta\beta_{O_{\Omega(k-1)}} + \Delta\beta_{\Omega(k-1)} - \Delta\beta_{\Omega k}
\end{cases} \tag{A13}$$

From Lemma 2, we have

$$\begin{cases}
\Delta z_{O_{\Omega(k-1)}} = \Delta z_{P_{r(k-1)}} + \Delta\alpha_{P_{r(k-1)}} y_{\Omega(k-1)} - \Delta\beta_{P_{r(k-1)}} x_{\Omega(k-1)} \\
\Delta\alpha_{O_{\Omega(k-1)}} = \Delta\alpha_{P_{r(k-1)}} \\
\Delta\beta_{O_{\Omega(k-1)}} = \Delta\beta_{P_{r(k-1)}}
\end{cases} \tag{A14}$$

Therefore, in GCS $\mathbf{B'}$ from Theorem 1, we have

$$\Delta P^{B'}_{O_{\Omega rk}} = J_{k-1} \begin{Bmatrix} \Delta P^{B'}_{O_{\Omega(k-1)}} \\ \Delta\Omega_{b(k-1)} \\ \Delta\Omega_{ak} \end{Bmatrix} \tag{A15}$$

where

$$J_{k-1}=\begin{bmatrix}
0 & 0 & 0 & & & \cdots & & & \cdots & & & \cdots & & & & 0\\
0 & 0 & 0 & & & \cdots & & & \cdots & & & \cdots & & & & 0\\
 & 0 & 1 & y_{\Omega_{(k-1)}} & -x_{\Omega_{(k-1)}} & 0 & 0 & 0 & 1 & 0 & 0 & 0 & 0 & 0 & -1 & 0 & 0 & 0\\
0 & 0 & 0 & 1 & 0 & 0 & 0 & 0 & 0 & 1 & 0 & 0 & 0 & 0 & 0 & -1 & 0 & 0\\
0 & 0 & 0 & 0 & 1 & 0 & 0 & 0 & 0 & 0 & 1 & 0 & 0 & 0 & 0 & 0 & -1 & 0\\
0 & 0 & 0 & & & \cdots & & & \cdots & & & \cdots & & & & 0
\end{bmatrix}_{3\times 18}$$

From Lemma 2, the deviation of any point on the feature plane Ω_k, can be obtained with $\bar{Q}$ and $\Delta P^{B'}_{O_{\Omega rk}}$ in GCS $\mathbf{B}'$. And, in turn, it can also be represented in GCS **B** and **A** through the transformation of $\bar{Q}^{-1}$, $\bar{\Phi}^{-1}$, respectively. It implies that once the virtual locating points are selected on mating feature k (Fig. 8) their deviations in GCS **A** can be obtained with the aforementioned transformations and treated as the generalized fixture errors. Combining these transformations into Eq. (6), we can actually obtain $\bar{J}_{k-1}$ for the generalized fixture. Detailed derivation of the explicit expressions is omitted for simplicity.

References

[1] Ceglarek, D., and Shi, J., 1995, "Dimensional Variation Reduction for Automotive Body Assembly: A Case Study," Manuf. Rev., **8**(2), pp. 139–154.

[2] Ceglarek, D., Huang, W., Zhou, S., Ding, Y., Ramesh, K., and Zhou, Y., 2004, "Time-Based Competition in Manufacturing: Stream-of-Variation Analysis (SOVA) Methodology—Review," Int. J. Flex. Manuf. Syst., **16**(1), pp. 11–44.

[3] Agrawal, R., Lawless, J. F., and Mackay, R. J., 1999, "Analysis of Variation Transmission in Manufacturing Processes—Part II," J. Quality Technol., **31**(2), pp. 143–154.

[4] Hsieh, C. C., and Oh, K. P., 1996, "Simulation and Optimization of Assembly Processes Involving Flexible Parts," ASME J. Manuf. Sci. Eng., **118**(3), pp. 377–382.

[5] Camelio, J. A., and Hu, S. J., 2004, "Multiple Fault Diagnosis for Sheet Metal Fixtures Using Designated Component Analysis," ASME J. Manuf. Sci. Eng., **126**(1), pp. 91–97.

[6] Chang, M., and Gossard, D. C., 1997, "Modeling the Assembly of Compliant, Non-Ideal Parts," Comput.-Aided Des., **29**(10), pp. 701–708.

[7] Ceglarek, D., and Shi, J., 1998, "Design Evaluation of Sheet Metal Joints for Dimensional Integrity," ASME J. Manuf. Sci. Eng., **120**, pp. 452–460.

[8] Ding, Y., Ceglarek, D., and Shi, J., 2002, "Design Evaluation of Multi-Station Manufacturing Processes by Using State Space Approach," ASME J. Mech. Des., **124**(4), pp. 408–418.

[9] Huang, W., 2004, "Methodologies for Modeling and Analysis of Stream-of-Variation in Compliant and Rigid Assembly," Ph.D. thesis, University of Wisconsin-Madison.

[10] Huang, W., and Ceglarek, D., 2005, "Statistical Modal Analysis Methodology for Form Error Modeling," IIE Trans., in review.

[11] Jin, J., and Shi, J., 1999, "States Space Modeling of Sheet Metal Assembly for Dimensional Control," ASME J. Manuf. Sci. Eng., **121**, pp. 756–762.

[12] Mantripragada, R., and Whitney, D. E., 1998, "Modeling and Controlling Variation in Mechanical Assemblies Using State Transition Models," *Proc. of 1998 IEEE Int. Conf. on Robotics & Automation*, Leuven, Belgium, pp. 219–226.

[13] Shalon, D., Gossard, D., Ulrich, K., and Fitzpatrick, D., 1992, "Representing Geometric Variations in Complex Structural Assemblies on CAD Systems," *ASME Advances in Design Automation*, ASME, New York, Vol. 2, pp. 121–132.

[14] Chase, K. W., Magleby, S. P., and Glancy, C. G., 1998, "A Comprehensive System for Computer-Aided Tolerance Analysis of 2D and 3D Mechanical Assemblies," *Geometric Design Tolerance: Theories, Standards and Applications*, Chapman and Hall, London, pp. 294–307.

[15] Gao, J., Chase, K. W., and Magleby, S. P., 1998, "General 3-D Tolerance Analysis of Mechanical Assemblies With Small Kinematic Adjustments," IIE Trans., **30**, pp. 367–377.

[16] Hong, Y. S., and Chang, T.-C., 2002, "A Comprehensive Review of Tolerancing Research," Int. J. Prod. Res., **40**(11), pp. 2425–2459.

[17] Ramesh, R., Mannan, M. A., and Poo, A. N., 2000, "Error Compensation in Machine Tools—A review, Part I: Geometric, Cutting-Force Induced and Fixture Dependent Errors," Int. J. Mach. Tools Manuf., **40**, pp. 1235–1256.

[18] Chou, Y.-C., Chandru, V., and Barash, M. M., 1989, "A Mathematical Approach to Automatic Configuration of Machining Fixtures: Analysis and Synthesis," ASME J. Eng. Ind., **111**, pp. 299–306.

[19] Choudhuri, S. A., and De Meter, E. C., 1999, "Tolerance Analysis of Machining Fixture Locators," ASME J. Manuf. Sci. Eng., **121**, pp. 273–281.

[20] Huang, Q., Zhou, S., Shi, J., 2000, "Stream of Variation Modeling and Diagnosis of Multi-Station Machining Processes," *Proc. of 2000 ASME IMECE*, ASME, New York, MED-Vol. 11, pp. 81–88.

[21] Zhou, S., Huang, Q., and Shi, J., 2003, "State Space Modeling of Dimensional Variation Propagation in Multistage Machining Process Using Differential Motion Vectors," IEEE Trans. Rob. Autom., **19**(2), pp. 96–309.

[22] Huang, W., Lin, J., Kong, Z., and Ceglarek, D., 2007, "Stream-of-Variation (SOVA) Modeling—II: A Generic 3D Variation Model for Rigid Body Assembly in Multi-Station Assembly Processes," revised, ASME J. Manuf. Sci. Eng., to be published.

[23] Huang, W., Phoomboplab, T., and Ceglarek, D., 2006, "Explicit Yield Model (EYM) for Tolerance Synthesis of Large Scale Complex Assemblies," ASME Paper No. ASME MSEC2006-21074.

[24] Lawless, J. F., Mackay, R. J., and Robinson, J. A., 1999, "Analysis of Variation Transmission in Manufacturing Processes—Part I," J. Quality Technol., **31**(2), pp. 131–142.

[25] Huang, W., and Ceglarek, D., 2005, "Model Complexity Reduction in Stream-of-Variation Analysis for Compliant Sheet Metal Assembly," presented at the 2005 CIRP Seminar on Computer-Aided Tolerancing, Tempe, AZ, April 11–12, p. CIRP-2004-40.

[26] Merkley, K. G., 1998, "Tolerance Analysis of Compliant Assemblies," Ph.D. thesis, Brigham Young University.

[27] Huang, W., and Ceglarek, D., 2002, "Mode-Based Decomposition of Part Form Error by Discrete-Cosine-Transform With Implementation to Assembly and Stamping System With Compliant Parts," CIRP Ann., **51**(1), pp. 21–26.

[28] Camelio, J., 2002, "Monitoring and Diagnosis of Dimensional Variation for Assembly Systems With Compliant Parts," Ph.D. thesis, Dept. of Mech. Eng. & Applied Mechanics, University of Michigan, Ann Arbor.

[29] Asada, H., and By, A., 1985, "Kinematic Analysis of Workpart Fixturing for Flexible Assembly With Automatically Reconfigurable Fixtures," IEEE Trans. Rob. Autom., **34**(3), pp. 337–345.

[30] Cai, W., Hu, S. J., and Yuan, J. X. 1997, "A Variational Method of Robust Fixture Configuration Design for 3-D Workpieces," ASME J. Manuf. Sci. Eng., **119**, pp. 593–602.

[31] Huang, W., and Ceglarek, D., 2005, "Model Complexity Reduction in Stream of Variation for Compliant Sheet Metal Assembly," 9th CIRP Int. Seminar on Computer Aided Tolerancing, Arizona.

[32] Wang, M. Y., and Pelinescu, D. M., 2001, "Optimizing Fixture Layout in a Point Set Domain," IEEE Trans. Rob. Autom., **17**(3), pp. 312–323.

[33] Crane, III., C. D., and Duffy, J., 1998, *Kinematic Analysis of Robotic Manipulators*, Cambridge University Press, Cambridge, England.